INVESTIGATION OF PILLAR-ROOF CONTACT FAILURE IN NORTHERN APPALACHIAN STONE MINE WORKINGS

Gabriel S. Esterhuizen, *Mining Engineer*
Anthony T. Iannacchione, *Senior Scientist*
National Institute for Occupational Safety and Health
Pittsburgh Research Laboratory
Pittsburgh, Pennsylvania USA

ABSTRACT

The roof rock in underground limestone mines in Northern Appalachia can be subject to high horizontal stresses in spite of the shallow depth of the workings. The high stresses can cause roof stability problems. The National Institute for Occupational Safety and Health staff have observed a distinctive asymmetrical mode of failure at the pillar-roof contact in two underground stone mines, which is different from the typical failure mode observed in response to excessive levels of horizontal stress. A dip of greater than 5° was identified as a possible cause of this mode of failure. Numerical model experiments showed that an increase in the dip of the workings can cause an increase in the stress at the up-dip corner of the roof beam. A case study is presented in which failure at the pillar-roof contact was observed where the dip of the workings was 7° in a high horizontal stress field. Numerical modeling showed that the relatively small dip of the workings could have induced stresses changes in the immediate roof that would explain the failures. The model results also showed that this mode of failure is less likely to occur if the limestone pillars contain weak bedding planes that provide stress relief. In addition, the results showed that for the conditions at the case study site, the stress in the roof beam was not sensitive to the thickness of the roof beam or to the excavation span. The high horizontal stresses at this site are an important contributing factor to the observed failures.

INTRODUCTION

Northern Appalachian stone mines operate in limestone formations ranging from 7 m (22 ft) to over 20 m (70 ft) thick which are easily accessible by room and pillar mining methods. The roof stability in these mines may be affected by high horizontal stresses in spite of the low overburden depth (Iannacchione et al., 2002). The horizontal stresses can cause excessive deflection and buckling of the layered limestone roof beams and may result in collapse of the roof. The National Institute for Occupational Safety and Health (NIOSH) has observed a distinctive asymmetrical mode of failure at the pillar-roof contact in two underground stone mines, which is different from the roof failure mode commonly observed in response to excessive levels of horizontal stress. The cause of the asymmetrical roof failure is not apparent and has consequently resulted in unexpected ground control problems in stone mine workings. Roof failures have been the cause of 73% of all fatalities and 32% of lost work days in underground stone mines from 1983 through 2002 (Mine Safety and Health Administration (MSHA), 2004). The Pittsburgh Research Laboratory of NIOSH has therefore undertaken a program of research to better understand the conditions that result in this type of failure and the mechanisms involved, with the objective to facilitate safer mine layout designs and improve the safety of mine workers.

OBSERVED ROOF FAILURES

Geotechnical Setting

Failure at the pillar-roof contact has been observed at several underground limestone mines, two of which are reported on in this paper. The two mines are located in Pennsylvania, one in the Loyalhanna Limestone Formation along the Chestnut Ridge and the other in the Valentine Formation, in Central Pennsylvania. The geotechnical characteristics of these two formations are summarized in table 1. The table shows that the limestone formations are strong and in the case of the Loyalhanna, overlain by weak roof rocks. In the Loyalhanna Formation, roof stability is achieved by maintaining a stable roof beam to support the overlying weaker rocks.

Table 1. Summary geotechnical characteristics.

Formation	Dip	Thickness, m (ft)	Uniaxial compressive strength, MPA (psi)	Characteristics of roof rocks
Loyalhanna	Flat lying to 20°	12 up to 28 (39 to 92)	54 to 256 (7,800 to 38,500)	Low strength shale, siltstone and calcareous sandstone, 23-43 MPa (3,300-6,200 psi)
Valentine	40° to near vertical	Approxi-mately 21 (69)	100 to 145 (14,500 to 21,000)	Limestone of equal strength or stronger than the Valentine limestone

Field Stresses

Stress measurements and field observations have shown that the horizontal stresses in the Northern Appalachian limestone formations are typically much higher than the vertical stress. The

limestone mines are located in the mid-North American plate where high horizontal stresses have been measured in several limestone mines (Iannacchione et al., 2002) and in many of the area's coal mines (Mark & Mucho, 1994). Latest research has shown that the high horizontal stress may be explained by the effect of plate tectonics (Dolinar, 2003; Iannacchione et al., 2002). Tectonic loading is related to the movement of the North American plate as it is pushed away from the mid-Atlantic ridge. A constant strain field of between 0.45 and 0.75 millistrains is associated with the tectonic loading, which induces high horizontal stresses in the stiff limestone strata. High stresses are not necessarily present in all the limestone formations because local features such as outcropping and folding may have relieved the stresses over geological time (Iannacchione and Coyle, 2002). Table 2 summarizes the range of horizontal stresses measured by NIOSH in the Loyalhanna and Valentine limestone formations.

Table 2. Magnitude and direction of the maximum horizontal stress measured in Northern Appalachian limestone mines.

Formation	Magnitude of maximum horizontal stress , MPa (psi)	Orientation of maximum horizontal stress
Loyalhanna Limestone[1]	27.4 to 47.7 (3,970 to 6,910)	N60°E to N75°E
Valentine Limestone[2]	14.9 to 29.6 (2,170 to 4,300)	N80°E

[1]Iannacchione et al., 2003
[2]Dolinar, 2004

Typical Failure under High Horizontal Stress

The more typical roof failure mode observed in high horizontal stress conditions may be described as progressive shearing and buckling of individual rock layers in the roof. The failures are often preceded by excessive deflection of the roof beams, which may be associated with micro-seismic emissions. Collapse of the roof beams can be progressive in the vertical direction, with individual beds typically failing from the bottom up. Failure may progress over days, weeks or months until a stable rock layer is reached. Once a portion of the roof has failed, the failed zone tends to propagate laterally, in a direction perpendicular to the major horizontal stress. The propagation of this type of failure may be halted by a barrier pillar or a change in the pillar layout. Cable bolting has sometimes been successful in halting the propagation.

Asymmetrical Failure at the Pillar-Roof Contact

Pillar-roof contact failure differs from the typical failure mode described above because it is asymmetrical, usually occurring only along one edge of each pillar in an array of pillars. The failure is initially restricted to a small area around the pillar edge, but may propagate to the full collapse of an entire room. Figure 1 illustrates a typical example of pillar-roof contact failure. The failures all appeared to be caused by stress related damage of the intact rock. The mode of failure, whether tensile or compressive, was not always readily observable. In several cases the failed rock had been removed and the roof had been scaled back to a solid face, which precluded direct observation of the failure mechanism. Both cases of pillar-roof contact failure were associated with a dip of greater than 5°.

Potential Causes of Asymmetrical Failures at the Pillar-Roof Contact

Asymmetrical failure in the rock surrounding underground excavations is often caused by stresses that are not parallel to the excavation boundaries. In the relatively flat lying limestone formations, stress rotation may occur as the result of variable topography or faulting. Rapid changes in the depth of cover can result in changes in the orientation of the major principal stress. In addition, the dip of the workings can result in rotation of the excavations relative to the field stress. From observations, it appears that the dip of the workings was a contributing factor in both cases of pillar-roof contact failure studied.

Figure 1. Photograph showing failure at pillar-roof contact after loose rock has been removed and roof has been re-supported.

A further potential contributing factor to pillar-roof contact failure is lateral displacement of the roof relative to the floor. Observations have shown that lateral displacements can occur between different rock beds in the roof, floor and within limestone pillars. Such movements can be expected to cause asymmetrical loading of the rock around the excavations.

ANALYSIS

The effect of dip on roof stability was selected for further analysis. The mine in the Loyalhanna Formation was selected as a case study because the dip appeared to be the only variable that differentiated the areas that experienced pillar-roof contact failure from areas that did not. The objective of the case study was to determine whether the relatively minor dip of the workings could have been responsible for the observed failures.

The pillar-roof contact failure observed at the mine in the Valentine Formation was complicated by the presence of an anomalous geological structure in addition to the dip, and was therefore excluded from the analyses.

Site Description

The case study mine is located in the Loyalhanna Formation which is nearly horizontal in the greater proportion of the workings but increases to 7° in the south-western part of the mine. The Loyalhanna formation in this area is between 17 m (55 ft) and 20 m (65 ft) thick. The limestone is massive, fine to medium grained with cross beds and strong, discontinuous bedding layers in the main body of the formation. The upper 3 m (10 ft) of the formation contains well developed laminations and alternating layers of weaker and stronger limestone, sandstone and shale. The immediate roof rocks are fine to medium grained sandstone but may also contain interbedded shale and limestone bands of the Mauch Chunk Formation. The RQD in the layered upper portion of the limestone formation is typically 85-95% increasing to 100% in the main body. At the base of the pillars in benched areas the floor rocks are a fine to coarse grained Pocono sandstone occasionally with a weak shale contact. RQD values in the floor are in the range of 60% to 90%. The Rock Mass Rating (RMR) (Bieniawski, 1989) of the massive limestone is in the range of 85 to 90 units. The mine exhibits many of the characteristic signs of excessive horizontal stress conditions. Mapping of roof damage has confirmed the presence of sporadic roof shearing and occasional massive directional roof falls. Most of the roof falls are oval in shape with the long axis in the N30°W direction.

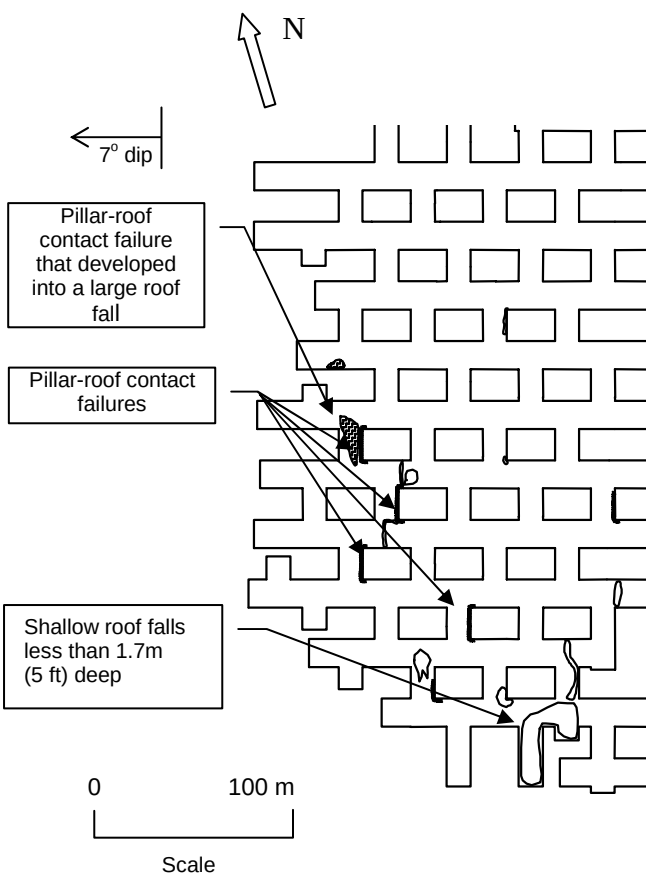

Figure 2. Plan showing layout of pillars and location of pillar-roof contact failures at case study site.

Asymmetrical failures at the pillar-roof contact were observed only in the southwestern part of the mine where the dip is gradually increasing. Figure 2 shows a plan view of a portion of the workings and the locations of pillar-roof contact failures as well as other roof failures. At one of the locations, the pillar-roof contact failure progressed into a massive directional failure. In this area the major horizontal stress appears to be oriented at approximately N80°W, parallel to the dip of the limestone. The change in orientation is apparent from major roof falls which are oriented along the strike of the workings in this area. Further indirect evidence of the major horizontal stress parallel to the dip is the dip-symmetry of the pillar-roof contact failures.

In the area of interest, the rooms are developed 13.7 m (45 ft) wide and the development mining height is typically 8 to 10 m (26 to 32 ft). The pillars are rectangular, having a length of 27.4 m (90 ft) parallel to the dip and a width of 15.2 m (50 ft). Approximately 2.4 m (8 ft) of limestone is left between the roof and the first weak layer to provide a stable roof beam. However, owing to the variable composition of the upper part of the Loyalhanna Formation, the roof may consist of alternating layers of strong and weak limestone, calcareous limestone and shale and clay bands.

Method of Analysis

All the analyses were carried out using the FLAC two-dimensional finite difference code (Itasca Consulting, 2000). The code allows mining sequences, gravity and tectonic loading as well as post failure behavior of rock to be modeled satisfactorily. The strain softening and ubiquitous joint features of the code were used to simulate post failure weakening of the rock as well as the effect of laminations in the limestone and the surrounding rocks.

A series of three-dimensional analyses were initially carried out to determine the validity of using two-dimensional models. It was found that two-dimensional models provide acceptable results of roof behavior near the center line of the pillars, which is the zone of interest of this study. The two-dimensional models do not provide any information on roof stability in the intersections. Two-dimensional models allow greater detail of roof layering and stress changes to be modeled than would be practical using three-dimensional models.

A parametric study of the effect of dip on stability of the roof was first carried out using the two-dimensional models. This was followed by a more detailed back analysis of the conditions in the case study area. Further analyses were carried out to investigate the effect of changes in the roof beam thicknesses and changes in the room width on roof stability. Finally an analysis was carried out in which the limestone pillars were assumed to contain two weak bedding planes, which allowed the horizontal stresses to be relieved. Since the immediate roof beam is essentially subject to uniaxial loading by the horizontal stress, the horizontal stress was used as an indicator of the potential for failure at the pillar-roof contact.

Parametric Study of Dip Effects

The parametric study was carried out to assess the effect of an increase in the dip on roof stability and the potential for pillar-roof contact failure. A base case two-dimensional FLAC model was set up to simulate the mining of a series of rooms in a 20 m (66 ft) thick limestone bed with a nominal depth of cover of 100 m (330 ft). The contact between the top of the limestone and the overburden was simulated as a weak interface, which is free to slide if the frictional resistance is overcome. The model layout,

showing the room, pillars and location of the weak interface is presented in figure 3. The material properties were selected to represent typical Loyalhanna limestone and the surrounding weaker rocks. Table 3 lists the material properties used in the basic model setup. The model was loaded in the vertical direction by gravity. The horizontal stresses were initialized to simulate the effects of constant tectonic strain, varying between 0.1 and 0.4 millistrain. The horizontal stress in the stiff limestone was always higher than in the softer surrounding rocks owing to the constant tectonic strain field. In these models the rock was assumed to be linearly elastic, so that shedding of stresses due to rock failure would not occur.

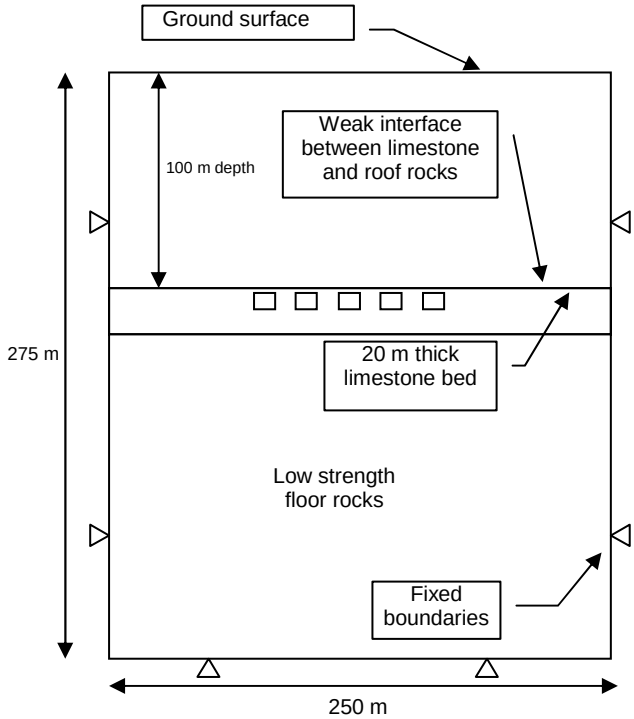

Figure 3. Numerical model layout showing location of rooms and pillars in the limestone formation.

Table 3. Base case material properties used in FLAC models.

Material	Bulk modulus, GPa (psi)	Shear modulus, GPa (psi)
Loyalhanna Limestone	49.2 (7.1 x 10^6)	37.0 (5.4 x10^6)
Overburden	2.2 (320,000)	1.6 (232,000)
Floor rock	7.6 (1.1 x 10^6)	5.7 (826,000)

The effect of an increase in the dip of the workings on stresses in the roof was assessed by changing the dip of the limestone in the model to 5, 10 and 15°, see figure 4.

The results of an analysis in which the horizontal stress in the limestone was 25 MPa (3,620 psi) (corresponding to a tectonic strain of 0.36 millistrain) are presented in table 4. These results show that the stress at the down-dip corner of the roof tends to decrease with increasing dip, while the stress at the upper corner increases. The changes in stress are relatively small. This implies that failure will only be caused by an increase in dip if the roof is already highly stressed and is near the point of failure. Under such a scenario, an increase in dip may initiate asymmetrical failure at the pillar roof contact on the up-dip side of a room.

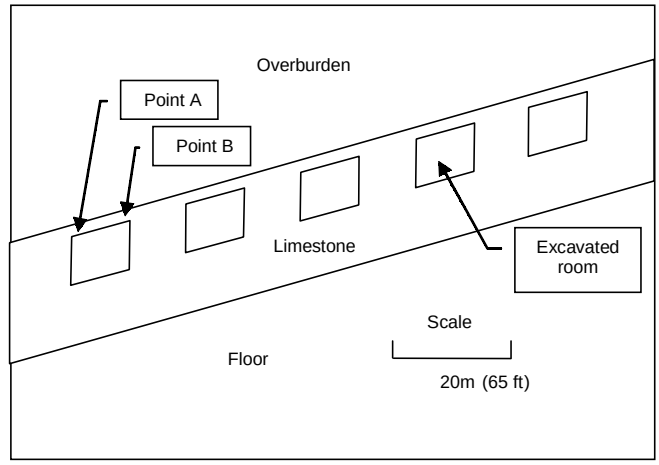

Figure 4. Detail of numerical model showing dipping limestone formation and location of Points A and B for assessment of stresses in the roof beam.

Table 4. Effect of dip on horizontal stresses in the immediate roof.

Dip of limestone formation	Percentage change in horizontal stress at A[1] (negative indicates decrease)	Percentage change in horizontal stress at B[1]
5°	-4.0%	+4.6%
10°	-10.4%	+7.9%
15°	-18.7%	+9.4%

[1]Refer to figure 4 for location of points A and B.

Back Analysis of Observed Failures

A detailed FLAC model of three rooms and the four adjacent pillars was used to back analyze the observed pillar-roof contact failures. The strain-softening ubiquitous joint constitutive model in FLAC was used to simulate the effect of layering of the rocks. This allows initial rock yield to occur and stresses to be shed as the failure progresses. A portion of the FLAC model is presented in figure 5, which shows the detail of the layering of the limestone and weaker overburden materials. The strength properties of the limestone rocks and the weak and strong roof beds are listed in table 5. The large scale rock strengths of the limestone and surrounding rocks were reduced by 0.58 from the laboratory determined strength values to account for the difference in strength of laboratory size specimens relative to the field scale, after Hoek and Brown (1980). The main body of the limestone was modeled as a massive unit, without any bedding weaknesses. The effect of weak bedding layers within the limestone pillars was evaluated separately.

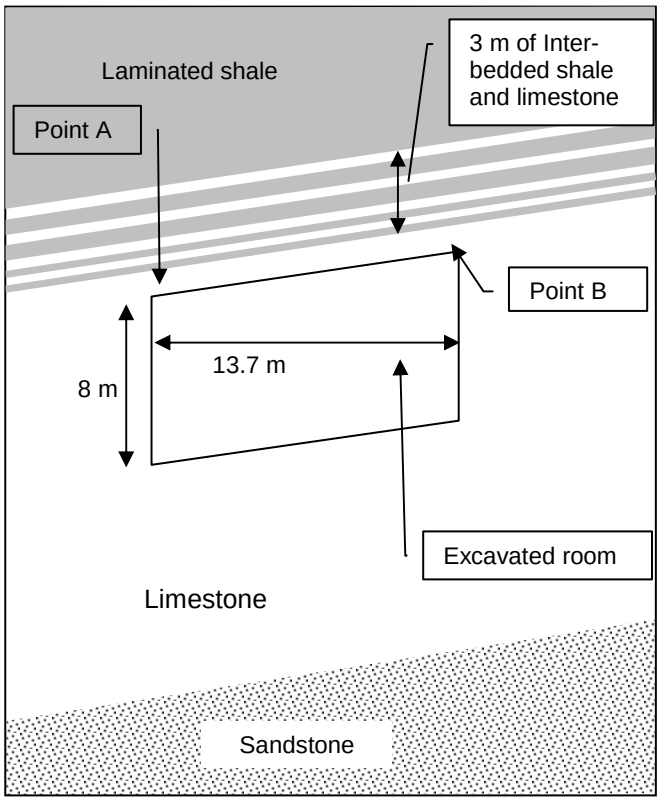

Figure 5. Detail of the numerical model used to assess the effect of dip on roof stability for the case study site. The locations of point A and B for assessment of roof stability are shown.

Table 5. Properties of limestone and bedding in the upper 3 m (10 ft) of the limestone formation used in the FLAC models.

Material	Rock cohesion, MPa (psi)	Rock friction angle	Rock tensile strength, MPa (psi)	Bedding cohesion, MPa (psi)	Bedding friction angle
Massive limestone	18 (2,610)	45°	8.0 (1,160)	-	-
Strong beds	12 (1,740)	35°	2.5 (360)	6.0 (870)	25°
Weak beds	4 (580)	25°	0.1 (14)	1.0 (145)	25°

The stresses in the model were initialized so that the horizontal stress depended on the stiffness of the rock layers and the vertical stress was dependent on the depth below the ground surface. The limestone horizontal stress of 35 MPa (5,070 psi) was selected to simulate a horizontal tectonic strain of 0.5 millistrain.

Stresses in the Roof Beam

For the initial analysis, the thickness of the solid limestone roof beam over the room was set to 1.2 m (4 ft), resulting in a total thickness of limestone and overlying interbeds of 4.2 m (14 ft).

The horizontal stresses in the rock surrounding the room are presented in figure 6 which clearly shows the asymmetrical nature of the stress distribution. The average horizontal stress in the roof beam increased considerably above the tectonic stress in the limestone, being in the range of 50-60 MPa (7,250-8,700 psi) at center span while the tectonic stress was 35 MPa (5,070 psi). The maximum horizontal stress values in the roof beam are found near the corners of the room. The horizontal stresses adjacent to the downdip corner (Point A) and updip corner of the roof (Point B) were 73.5 MPa (10,660 psi) and 88.5 MPa (12,830 psi), respectively.

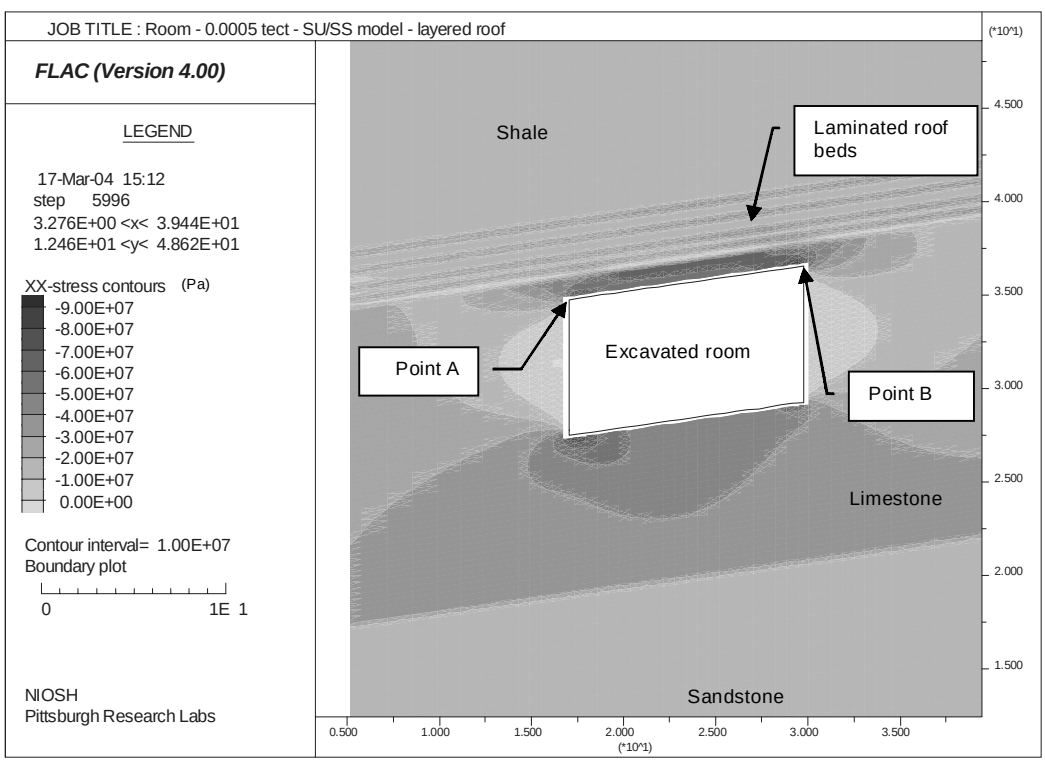

Figure 6. FLAC plot showing horizontal stress distribution around a room with interbedded roof rocks in massive limestone. Contour intervals are 10 MPa (1,450 psi). The tectonic stress was 0.5 millistrain.

The stress near the updip corner of the room is therefore approximately 20% higher than at the downdip corner. This is consistent with the observations that showed that failure initiated at the up-dip corner of the rooms and confirms that failures at the pillar-roof contact are likely to be the result of asymmetrical stresses owing to the dip of the workings.

Two additional sets of analyses were carried out to determine if the roof beam stability could be improved by changing the thickness of the roof beam or by reducing the width of the rooms. Conventional roof beam mechanics, in which beams are loaded by their own weight, such as the Voussoir beam method (Beer and Meek, 1982) or simple elastic beam formulations (Obert and Duvall, 1967), indicate that beam stability is greatly enhanced by a reduction in the beam span or by an increase in the beam thickness. However, in this case where the beams contain high horizontal stresses, the effects of changes in the beam dimensions are dominated by re-distribution of the horizontal stress, and were found to be contrary to expectations.

Results for Variable Roof Beam Thicknesses

The thickness of the beam between the roof of the workings and the first weak interbed was varied between 0.6 m (2 ft) to 2.4 m (8 ft) to determine whether stability would be enhanced by increasing the beam thickness. The total thickness of the roof beam from the upper limestone interbed to the roof was therefore varied between 3.6 m (11.8 ft) and 5.4 m (17.7 ft).

The results are presented in table 6, which show that the stress in the roof beam is not sensitive to the beam thickness until the beam is reduced to only 0.6 m (2 ft). Inspection of the model results showed that this sudden increase in the stress is related to the initiation of failure in the overlying shale which causes downwards deflection of the roof beam and induces high stresses at the excavation corners. The results illustrate the potentially complex behavior of the roof rocks and the difficulty in estimating stability without detailed knowledge of the roof beam thickness and strength properties of the various rock layers.

Table 6. Horizontal stress in the roof beam for different roof beam thicknesses in massive limestone.

Limestone roof beam thickness, m (ft)	Horizontal stress at A, MPa (psi)	Horizontal stress at B, MPa (psi)
0.6 (2)	95.4 (13,830)	104.8 (15,200)
1.2 (4)	73.5 (10,660)	88.5 (12,830)
1.8 (6)	71.1 (10,310)	90.9 (13,180)
2.4 (8)	69.0 (10,000)	92.5 (13,410)

Results for Variable Room Widths

The effect of changing the room width was evaluated by reducing the room width in the model from 13.7 m (45 ft) down to 8.2 m (27 ft) and comparing the stresses in the roof beam. The results are summarized in table 7, which shows that for the high horizontal stress conditions at the mine site, a reduction in room width does not necessarily result in a reduction in the horizontal stress of the roof beam. The reason for this unusual behavior is that the roof beam relieves stress by vertical deflection. A thicker beam is less able to deflect and is therefore unable to relieve the high horizontal stress. This is contrary to the behavior of beams that deflect under their own weight.

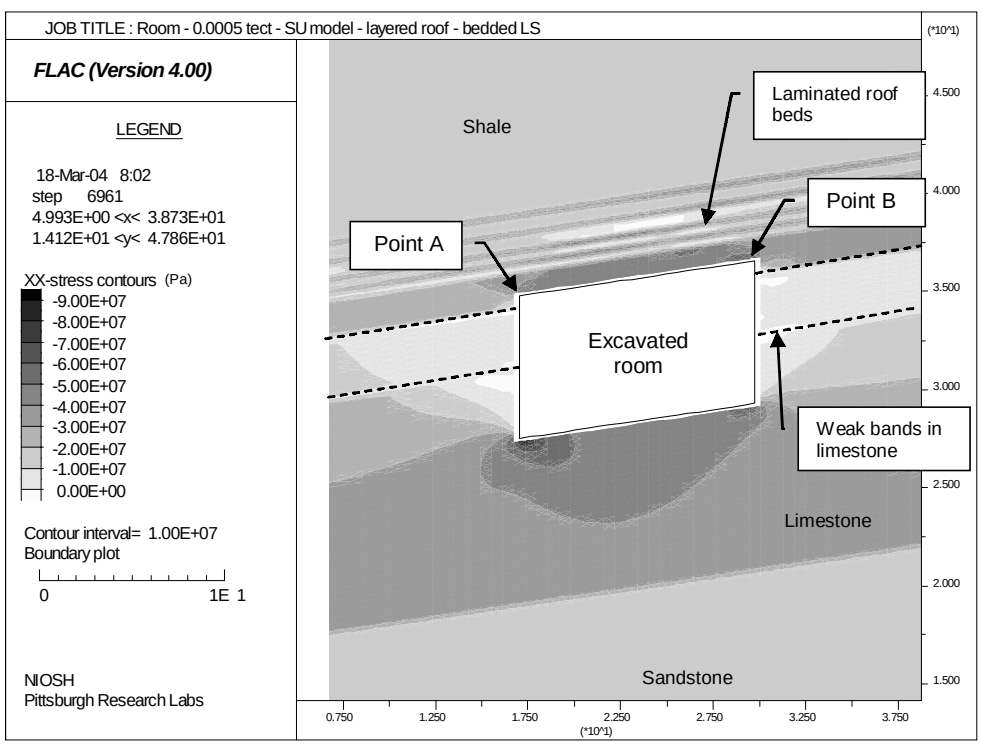

Figure 7. FLAC plot showing horizontal stress distribution around a room with interbedded roof rocks in limestone containing weak bands. Contour intervals are 10 MPa (1,450 psi).

Table 7. Horizontal stress in the roof beam for different room widths in massive limestone.

Room width, m (ft)	Horizontal stress at A, MPa (psi)	Horizontal stress at B, MPa (psi)
13.7 (45)	73.5 (10,660)	95.6 (13,860)
11.9 (39)	75.4 (10,930)	97.6 (14,150)
10.1 (33)	79.9 (11,590)	102.5 (14,862)
8.2 (27)	84.4 (12,240)	108.5 (15,730)

Results for Limestone Pillars Containing Weak Bands

The above analyses demonstrated the importance of layering in the roof and stress relief by sliding along weak beds. The fact that failure at the pillar-roof contact did not occur at all the pillars was thought to be related to a stress relief mechanism, which may be associated with weak bands in the limestone. Consequently, a model was set up to simulate limestone pillars that contain two weak bands near mid-height. Figure 7 shows the horizontal stress distribution in such a pillar, and can be directly compared to figure 6. It can be seen that stress relief along the weak bands in the pillar result in a significant reduction in the stress in the roof. The horizontal stress at Point A reduces from 73.5 MPa (10,660 psi) to 54.3 MPa (7,870 psi), which is a 26% reduction. The horizontal stress at Point B reduces from 95.6 MPa (13,860 psi) to 65.1 MPa (9,440 psi), which is a 32% reduction.

The results demonstrate that the presence of weak bands in the limestone may act as a stress relief mechanism. Limestone containing strong and discontinuous bedding would therefore be more prone to stress related roof failures than a limestone with weak bedding planes.

CONCLUSIONS

Field observations combined with numerical model studies indicate that asymmetrical failure at the pillar-roof contact in highly stressed limestone formations can be caused by stress rotation relative to the excavation boundaries owing to the dip of the workings. An increase in the dip of the workings results in increased stresses in the up-dip corner of a room, which may initiate failure at the pillar-roof contact, similar to the failures observed in the field.

A case study demonstrated that failures observed at the pillar-roof contact on the up-dip side of rooms dipping at 7° may be satisfactorily explained by the elevated stresses caused by the dip of the workings. Numerical models showed that, for the conditions at the case study site, the stress at the up-dip side of a room are typically 20% higher than the down-dip side, in spite of the relatively minor dip of the workings. In addition, the results showed that:

1. The horizontal stress in the limestone roof beam was not sensitive to the thickness of the beam for beam thicknesses of 0.6 m (4 ft) or greater.
2. Failure of the weak shale that overlies the limestone has an unfavorable effect on the limestone roof beam stability.
3. Reducing the room width could cause an increase in the horizontal stress in the limestone roof beam and may bring the beam closer to failure. This phenomenon is the result of the initially high horizontal tectonic stress in the limestone.
4. Failure at the pillar-roof contact is more likely to occur in areas where the pillars consist of massive limestone than in areas where the limestone pillars contain weak bedding planes. The weak planes provide shear surfaces which relieve the high horizontal stresses.

The model results seem to indicate that increasing the room width might be a technique to reduce high horizontal stresses in the roof beam. However, the model did not consider all the factors that could affect roof stability, such as the effect of a loss of horizontal stress, the presence of jointing or other structures and the capability of the roof support system.

The study has shown that failure at the pillar roof contact can be linked to the high tectonic stresses in the stiff limestone roof rocks. Small changes in the orientation of the field stresses can initiate failure in the already highly stressed roof rocks.

REFERENCES

Beer, G. and Meek, J.L. (1982). Design Curves for Roofs and Hangingwalls in Bedded Rock Based on Voussoir Beam and Plate Solutions. Trans Inst. Min. Metall., Vol. 91, pp. A18-22.

Bieniawski, Z.T. (1989). Engineering Rock Mass Classifications. Wiley, New York.

Dolinar, D.R. (2003). Variation of Horizontal Stresses and Strains in Mines in Bedded Deposits in the Eastern and Midwestern United States. Proceedings, 22nd International Conference on Ground Control in Mining, WV University, Morgantown, WV, Aug. 5-7, pp. 178-185.

Dolinar, D.R. (2004) Personal communication, Pittsburgh.

Hoek, E. and Brown, E.T. (1980). Underground Excavations in Rock. Inst. Mining and Metallurgy, p.156.

Iannacchione, A.T., Dolinar, D.R. and Mucho, T.P. (2002). High Stress Mining Under Shallow Overburden in Underground U.S. Stone Mines. Proceedings, Intl. Seminar of Deep and High Stress Mining Brisbane, Australia: Australian Centre for Geomechanics, pp. 1-11.

Iannacchione, A.T. and Coyle, P.R. (2002). An Examination of the Loyalhanna Limestone's Structural Features and their Impact on Mining and Ground Control Practices. Proceedings, 21st International Conference on Ground Control in Mining, WV University, Morgantown, WV, Aug. 6-8, pp. 218-227.

Iannacchione, A.T., Marshall, T.E., Burke, L.M., Melville, R. and Litsenberger, J. (2003). Safer Mine Layouts for Underground Stone Mines Subjected to Excessive Levels of Horizontal Stress. *Mining Engineering*, April, pp. 25-31.

Itasca Consulting Group (2000). Fast Lagrangian Analysis of Continua, 2nd Edition, Minnesota.

Mark, C. and Mucho, T.P. (1994). Longwall Mine Design for Control of Horizontal Stress. U.S. Bureau of Mines Special Publication 01-94, New Technology for Longwall Ground Control, pp. 53-76.

MSHA (2004). Mining Industry Accident, Injuries, Employment and Production Statistics. Retrieved March 19, from http://www.msha.gov/ACCINJ/accinj.htm.

Obert, L. and Duvall, W.I. Rock Mechanics and the Design of Structures in Rock. John Wiley & Sons, New York, 1967, 650 pp.